NeuroImage: Clinical 36 (2022) 103174

Contents lists available at ScienceDirect

NeuroImage: Clinical

journal homepage: www.elsevier.com/locate/ynicl

Exploring biomarkers of processing speed and executive function: The role of the anterior thalamic radiations

Jennifer Ferris [a,b], Brian Greeley [a], Negin Motamed Yeganeh [c], Shie Rinat [a,b], Joel Ramirez [d,e], Sandra Black [d,e], Lara Boyd [a,b,c,*]

[a] Department of Physical Therapy, University of British Columbia, Vancouver, Canada
[b] Graduate Programs in Rehabilitation Sciences, University of British Columbia, Vancouver, Canada
[c] Djavad Mowafaghian Centre for Brain Health, University of British Columbia, Vancouver, Canada
[d] LC Campbell Cognitive Neurology Research Unit, Dr Sandra Black Centre for Brain Resilience and Recovery, Toronto, Canada
[e] Hurvitz Brain Sciences Research Program, Sunnybrook Research Institute, University of Toronto, Toronto, Canada

A B S T R A C T

Introduction: Processing speed and executive function are often impaired after stroke and in typical aging. However, there are no reliable neurological markers of these cognitive impairments. The trail making test (TMT) is a common index of processing speed and executive function. Here, we tested candidate MRI markers of TMT performance in a cohort of older adults and individuals with chronic stroke.

Methods: In 61 older adults and 32 individuals with chronic stroke, we indexed white matter structure with region-specific lesion load (of white matter hyperintensities (WMHs) and stroke lesions) and diffusion tensor imaging (DTI) from four regions related to TMT performance: the anterior thalamic radiations (ATR), superior longitudinal fasciculus (SLF), forceps minor, and cholinergic pathways. Regression modelling was used to identify the marker(s) that explained the most variance in TMT performance.

Results: DTI metrics of the ATR related to processing speed in both the older adult (TMT A: $\beta = -3.431$, $p < 0.001$) and chronic stroke (TMT A: $\beta = 11.282$, $p < 0.001$) groups. In the chronic stroke group executive function was best predicted by a combination of ATR and forceps minor DTI metrics (TMT B: $_{adjusted}R^2 = 0.438$, $p < 0.001$); no significant predictors of executive function (TMT B) emerged in the older adult group. No imaging metrics related to set shifting (TMT B-A). Regional DTI metrics predicted TMT performance above and beyond whole-brain stroke and WMH volumes and removing whole-brain lesion volumes improved model fits.

Conclusions: In this comprehensive assessment of candidate imaging markers, we demonstrate an association between ATR microstructure and processing speed and executive function performance. Regional DTI metrics provided better predictors of cognitive performance than whole-brain lesion volumes or regional lesion load, emphasizing the importance of lesion location in understanding cognition. We propose ATR DTI metrics as novel candidate imaging biomarker of post-stroke cognitive impairment.

1. Introduction

Cognitive impairment affects approximately 40 % of individuals who survive a stroke (Sexton, 2019). Specifically, processing speed and executive functions are often impaired after stroke (Knopman, 2009; Pohjasvaara, 2002), and are associated with poorer functional outcomes Barker-Collo et al., 2010, increased dependency Narasimhalu et al., 2011, and reduced employment (Mahon, 2020) in individuals with chronic stroke. Despite its high prevalence and clinical importance, we do not understand the patterns of brain damage associated with post-stroke cognitive impairment. The aim of this study was to identify clinically relevant brain-based biomarker(s) of cognition in individuals who have had a stroke. This work is in direct response to the Stroke Recovery and Rehabilitation Roundtable, which identified the discovery of brain-based biomarkers of cognition as a research priority (Boyd et al., 2017). As summarized by the Roundtable (Boyd et al., 2017), an effective cognitive biomarker could be used to predict cognitive outcomes in typical brain degeneration (i.e., aging), injury (i.e., stroke), and / or their interaction, to stratify patient subgroups in clinical trials of cognitive interventions, or to predict an individual's treatment response in rehabilitation. However, more preliminary cross-sectional work is needed to identify promising neuronal pathways or networks that relate to cognition, with MRI-based measures that can capture disease processes in these pathways.

In addition to stroke infarcts, concurrent aging and vascular neurodegeneration may also impact cognition post-stroke (Arsava et al., 2009). Declining processing speed and executive function in typical aging are strongly linked to white matter hyperintensities (WMHs)

* Corresponding author at: University of British Columbia, 212-2177 Wesbrook Mall, Vancouver, British Columbia V6T 2B5, Canada.
E-mail address: lara.boyd@ubc.ca (L. Boyd).

https://doi.org/10.1016/j.nicl.2022.103174
Received 20 April 2022; Received in revised form 8 August 2022; Accepted 27 August 2022
Available online 30 August 2022

(Debette and Markus, 2010), the most prominent manifestation of cerebral small vessel disease. In typical aging WMHs impact processing speed and executive functions more than any other cognitive domain (Vasquez and Zakzanis, 2015). Individuals who experience a stroke are more likely to have large WMH volumes (Wen and Sachdev, 2004), due to the shared cardiometabolic risk factors for large and small vessel cerebrovascular disease (Jeerakathil et al., 2004). Thus, stroke lesions occur over a background of WMHs, and the common neuropsychological profiles between individuals with stroke and WMHs implies that there may be similar neurobiological pathways that accompany these cognitive changes. Combining information from WMHs and overt stroke lesions could provide new insight into the neurological basis of cognitive impairment post-stroke.

In previous analyses of processing speed and executive function four frontal-subcortical white matter tracts have emerged as likely imaging marker candidates: the anterior thalamic radiations (ATR), superior longitudinal fasciculus (SLF), forceps minor of the corpus callosum, and cholinergic pathways of the basal forebrain. These tracts encompass frontal-subcortical white matter circuits that have a theoretical role in cognitive impairment in cerebrovascular disease (Tekin and Cummings, 2002). Additionally, cholinergic signaling modulates executive function (Ballinger et al., 2016), and disruption to cholinergic pathways may contribute to cognitive impairment in cerebrovascular disease (Lim et al., 2014). The evidence for these regional markers of processing speed and executive function falls into two methodological categories. The first is region-specific lesion load, which measures the degree of overlap between a lesion mask and a white matter tract. WMH lesion load in the ATR (Biesbroek et al., 2016; Biesbroek et al., 2013; Lampe, 2019), SLF (Biesbroek et al., 2016; Biesbroek et al., 2013), and forceps minor (Duering et al., 2013; Duering et al., 2014) relate to processing speed and executive function in older adults. Stroke lesion load in cholinergic pathways relates to processing speed and executive function in individuals with chronic stroke (Muir et al., 2015). The second methodological tool is regional white matter microstrcuture measures from diffusion tensor imaging (DTI). DTI studies have shown some concurrence with regional lesion load studies; processing speed and executive function related to ATR (Cremers, 2016; MacPherson et al., 2017) and SLF (Cremers, 2016) microstructure in older adult with WMHs, and SLF microstructure in individuals with subacute stroke (Veldsman et al., 2020). In addition to employing different methodological techniques to characterize white matter damage, these previous studies have significant heterogeneity in the types of cognitive assessments used and the regions of interest examined. Moreover, most previous work that has observed relationships between ATR (Biesbroek et al., 2016; Biesbroek et al., 2013; Lampe, 2019; MacPherson et al., 2017), SLF (Biesbroek et al., 2016; Biesbroek et al., 2013), and forceps minor (Duering et al., 2014) were hypothesis-free, voxel-wise analyses, whereas a whole-tract approach could more feasibly be used as a clinically relevant cognitive biomarker. Thus, it is unknown which specific region (e.g., ATR, SLF, forceps minor, or cholinergic pathways) and which index of structural damage (e.g., lesion load, DTI, or a combination of the two) are the most sensitive predictors of processing speed and executive function.

In this study we indexed processing speed and set shifting, a component of executive function, with the trail making test (TMT), a widely used (Tombaugh, 2004) and sensitive (Rasmusson et al., 1998) neuropsychological assessment. The TMT is composed of two subtests, which are composite cognitive measures. TMT A measures processing speed, including psychomotor speed and visual search (Crowe, 1998). TMT B is more cognitively demanding than TMT A. TMT B relies on higher-order executive functions such as set shifting, in addition to processing speed and visual search components (Crowe, 1998). Additionally TMT B-A can be computed to eliminate the processing speed components in the TMT and specifically index set shifting abilities (Stuss, 2001). The TMT is a useful clinical screening tool; TMT performance predicts conversion from mild cognitive impairment to overt dementia (Ewers, 2012), and TMT B is a predictor of fitness to drive after stroke (Devos et al., 2011). We employed the TMT, adapted for a robotic device (Mang et al., 2019), to comprehensively test relationships between frontal-subcortical white matter pathways and components of TMT performance.

Here we present a systematic analysis of a select number of candidate white matter biomarkers shown to be involved in processing speed and executive function. This analysis was specifically designed to resolve the heterogeneity in the cognitive biomarker literature regarding the choice of white matter region and structural metrics employed as promising biomarkers of cognition. We investigated four candidate brain-based biomarkers of processing speed and executive function (ATR (Duering et al., 2014; MacPherson et al., 2017), SLF (Veldsman et al., 2020; Perry et al., 2009), forceps minor (Duering et al., 2014), and cholinergic pathways (Muir et al., 2015) in a cohort of older adults and individuals in the chronic phase of stroke recovery.We indexed structural damage in these pathways using two methods: region-specific lesion load (for both WMH and stroke lesions) and DTI microstructure. We hypothesized that regional white matter markers would explain more variance in TMT performance than whole-brain lesion volumes, but we did not have specific hypotheses about which white matter tracts(s) or structural marker(s) (lesion load vs DTI microstructure) would emerge as the best candidate biomarkers of TMT performance.

2. Methods

2.1. Participants

This study was a secondary analysis of pooled data from the baseline assessments of two research studies conducted by the UBC Brain Behaviour Lab. We included 62 healthy older adults and 34 individuals with chronic stroke who received multimodal neuroimaging between 2016 and 2020. Participants were considered eligible if they were between 40 and 80 years old, and for the stroke group if they were in the chronic phase of stroke recovery (>6 months post a clinically diagnosed stroke). Participants were ineligible if they: 1) had a history of seizure/epilepsy, head trauma, a major psychiatric diagnosis, neurodegenerative disorders, or substance abuse, or 2) reported any contraindications to MRI. General cognitive performance was assessed with the Montreal Cognitive Assessment (MoCA) (Nasreddine, 2005). Informed consent was obtained for each participant in accordance with the Declaration of Helsinki. The University research ethics boards approved all aspects of the study protocol.

2.2. Trail making test

All participants completed the TMT on a Kinesiological Instrument for Normal and Altered Reaching Movement (KINARM) end-point device (B-KIN Technologies, Kingston, Ontario). The KINARM TMT is part of the KINARM Standard Tests™ testing battery, and is a robotic adaptation of the pen-and-paper TMT task (Nasreddine, 2005) (Fig. 1). Robotic assessment tools have advantages as objective, reliable and sensitive measures of behaviour (Scott and Dukelow, 2011). The KINARM endpoint robot requires participants to grip and hold a frictionless manipulandum; this version of the TMT avoids any confound in TMT performance from reduced fine motor control or dexterity (Schear and Sato, 1989). The KINARM TMT-B had comparable test–retest reliability to the pen-and-paper TMT-B in a cohort of young adult athletes (Mang et al., 2018).

Participants were seated, centered in the KINARM workspace. Participants grasped and moved the end-point handles during the task, with the hand represented by a small white circle as a cursor. TMT targets were displayed on the working side of the KINARM workspace, and participants were instructed to move their hand through the series of targets as quickly and accurately as possible. Regardless of the task, the first target was always numbered 1 and illuminated yellow. As

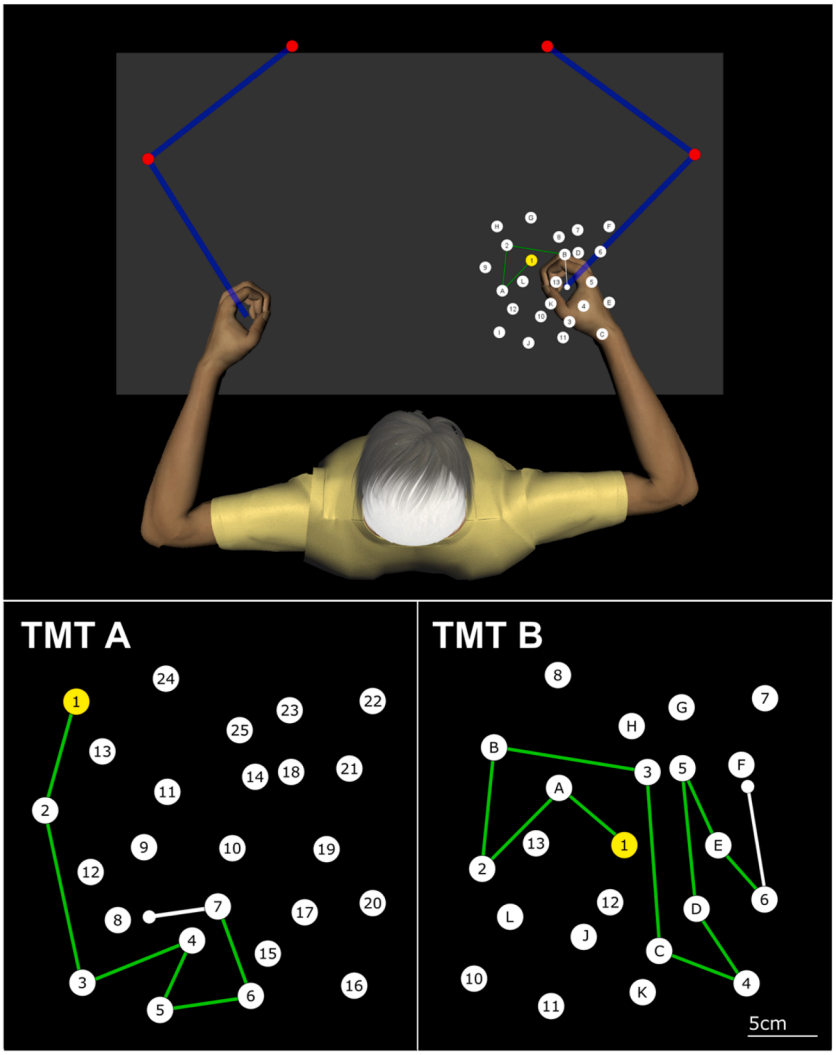

Fig. 1. Trail making test experimental setup Top panel: schematic of the KINARM-adapted trail making task (TMT), showing relative position of the participant and the TMT targets. Participants grabbed an endpoint robotic manipulandum to move their cursor (small white circle) through the TMT targets. Bottom panel: TMT A and B. The start target appeared yellow. Participants moved the cursor between targets, connecting numbers sequentially for TMT A (left) and alternating between numbers and letters in ascending order for TMT B (right). White lines appeared connecting targets mid-movement, which turned green once the participants contacted the next correct target.

participants moved from one correct target to the next correct target, the line connecting the two targets became fixed and turned green, whereas if participants made an error by moving to an incorrect target, the previously correct target turned red. If this occurred, participants returned to the last correct target (displayed in red) to resume the task. After the instructions and prior to starting the full task, all participants completed a short practice comprised of a five-target version of the task (e.g., 1–2-3–4-5 for TMT A; 1-A-2-B-3 for TMT B). Older adults completed the TMT using their dominant limb. Individuals with chronic stroke completed the TMT with their preferred limb, meaning the participants decided which limb would give the best possible performance on the TMT based on their individual motor abilities. For the majority of participants (n = 29) the preferred limb was the non-paretic limb. However, a small number of participants (n = 5) who had mild motor deficits (upper extremity FM range: 55 to 60) chose to complete the TMT with their right hand, which was both their stroke-affected hand and their dominant hand pre-stroke.

2.3. Trail making task A

The TMT A was comprised of 25 white circular targets numbered 1 to 25 (Fig. 1). Targets were randomly distributed in one of 8 possible random patterns. Participants were instructed to connect the targets in ascending numerical sequence as quickly and accurately as possible.

2.4. Trail making task B

The TMT B array was comprised of 25 white circular targets with numeric values from 1 to 13 and letter values from A to L (Fig. 1). Targets were randomly distributed in one of 8 possible random patterns. Participants were instructed to connect the numbers and letters in ascending alternating alpha-numeric order.

2.5. Outcome measures

We considered three standard TMT outcome measures of interest (Bowie and Harvey, 2006): total time to complete TMT A, total time to complete TMT B, and TMT B-A time. Total time was defined as the total time taken (seconds) to complete the TMT. The time started once the targets were presented on the screen and ended when the curser contacted the last target. TMT B-A was calculated by subtracting total TMT B time from total TMT A time.

2.6. MRI acquisition

MRI scans were acquired at the University of British Columbia MRI Research Centre on 3.0 T Phillips Achieva or Elition scanners (Philips Healthcare, Best, The Netherlands), with parallel imaging and an eight-channel and thirty-two-channel sensitivity encoding head coil, respectively. We acquired the following structural scans: 1) a 3D

magnetization-prepared rapid gradient-echo (MPRAGE) T1 anatomical scan (repetition time (TR)/time to echo (TE)/inversion time (TI) = 3000/3.7/905 ms, flip angle = 9°, voxel size = 1 mm isotropic, field of view (FOV) = 256 × 224 × 180 mm), 2) a fluid attenuated inversion recovery (FLAIR) scan acquired in the axial plane (TR/TE/TI = 9000/90/2500 ms, flip angle = 90°, voxel size = 0.94 × 0.94 mm FOV = 240 × 191 × 144 mm, slice thickness = 3 mm), and 3) a combined T2-weighted (T2) and proton density (PD) scan acquired in the axial plane (TR/TE1/TE2 = 2500/9.5/90 ms, flip angle = 90°, voxel size = 0.94 × 0.94 mm, FOV = 240 × 191 × 144 mm, slice thickness = 3 mm). For DTI data, a 3D high-angular resolution diffusion imaging (HARDI) scan was acquired across 60 non-collinear diffusion gradients (b-value = 700 s/mm^2, TR/TE = 7094/60 ms, voxel size = 2 mm, FOV = 224 × 224 × 154 mm, slice thickness = 2.2 mm), along with two unweighted (b0) diffusion volumes.

2.7. MRI preprocessing

Structural segmentation was performed with the Semi-Automated Brain Region Extraction (SABRE) and Lesion Explorer pipelines (Ramirez et al., 2011; Ramirez et al., 2020). Briefly, T1, FLAIR, T2 and PD scans were linearly co-registered and supratentorial cerebral tissue was segmented into cerebrospinal fluid (CSF; sulcal and ventricular), grey matter, normal-appearing white matter (NAWM), and WMHs. Stroke lesions were manually traced over co-registered T1 and FLAIR scans by a single experienced researcher (by J.K.F).

T1 images were skull-stripped using the FMRIB Software Library (FSL) Brain Extraction Tool (BET) (Smith, 2002). For stroke participants with large cortical lesions, BET often fails to identify the boundaries of the stroke lesion. To improve BET segmentation in the presence of large cortical lesions, stroke lesion masks were set to a voxel intensity roughly corresponding to grey matter and added to T1 scans prior to BET skull strip. The generated binarized BET mask was then used to mask out the original T1 image, to create a skull stripped unaltered T1 image where BET follows the boundaries of the stroke lesion. BET skull strips were visually checked by a single researcher (J.K.F.). T1 scans were non-linearly registered to MNI space using FSL's FNIRT (Andersson et al., 2007). To minimize warping from stroke lesions in non-linear registrations, stroke lesion masks were flipped across the sagittal midline and a copy of contralesional tissue was created, which was then used to fill in the stroke region on the T1 scan prior to non-linear registration (Nachev et al., 2008). WMH masks were incorporated in the MNI registration using a cost-function mask, and registration was performed with a warp resolution of 5 mm. The quality of MNI registrations was visually confirmed by a single rater (J.K.F.).

Diffusion images were preprocessed with FSL's diffusion toolbox (FDT) (Smith et al., 2004). Briefly, DTI data were corrected for motion and eddy-current distortions, and the unweighted DTI volume was skull-stripped with BET. Fractional anisotropy (FA) and mean diffusivity (MD) maps were generated using DTIFIT. T1 scans were registered to the unweighted DTI volume using FSL's FLIRT (Jenkinson et al., 2002) by a rigid-body linear registration with a correlation ratio cost function. Registration quality was visually checked by a single rater (J.K.F.) and manually adjusted where necessary with tkregister from Freesurfer v.6.0.

2.8. Regions of interest

ATR, SLF, and forceps minor tracts were taken as regions of interest (ROIs) from the JHU white matter atlas (Hua et al., 2008) and binarized with a probability threshold of 0.1 (Biesbroek et al., 2016; Duering et al., 20112011). The left and right hemispheres of ATR and SLF were combined to create a single bilateral ROI for each region in order to reduce the number of comparisons in preliminary statistical investigations. To calculate regional lesion load: WMH and stroke masks were moved to MNI space, and we calculated the overlap between the lesion mask and the ROI. We then computed a weighted lesion load for each ROI, according to previously published methods (Feng, 2015). For lesion load calculations, ROIs were sliced in the plane that corresponded to capturing the cross-sectional area of each ROI (coronal plane for ATR and SLF; sagittal plane for forceps minor). To calculate regional DTI metrics: ROIs were moved to T1 space and eroded to subject-specific white matter anatomy by removing voxels containing grey matter or cerebrospinal fluid. Next, ROIs were moved to DTI space and mean FA and MD were extracted. Based on the Cholinergic Pathways Hyperintensities Scale (CHIPS) (Bocti et al., 2005), lateral cholinergic fiber projections from the most inferior point of the external capsule and extending to the center of the centrum semiovale (McNeely, 2015) were automatically parcellated from the SABRE atlas (Dade et al., 2004); and WMH and stroke lesion load was calculated in the cholinergic pathways, according to previously published methods (McNeely, 2015). DTI measures were not extracted from cholinergic pathways because this area contains unmyelinated white matter fibers (Selden et al., 1998) and overlaps with the trajectory of the SLF (Muir et al., 2015). See Fig. 2 for an overview of ROIs included in the analysis.

2.9. Statistics

Statistical analyses were performed with R (programming environment v4.0.4); the alpha threshold for significance was set at $p < 0.05$. Whole-brain lesion volumes and tract-specific lesion load measures were positively skewed and were log-transformed prior to statistical analysis. Relationships between imaging markers and TMT performance were tested separately for each group (older adults, chronic stroke), and outcome measure (TMT A, TMT B, and TMT B-A). First, we performed exploratory Spearman's correlations between cognitive outcome measures and imaging metrics (WMH lesion load, stroke lesion load, FA, and MD) for each ROI (ATR, SLF, forceps minor, and cholinergic pathways). Next, we entered any variables that significantly correlated with the TMT outcome measure into linear regression models, to test which regional markers, or combination of markers, explained the most variance in TMT performance. Regression models were adjusted for age and time post stroke (for chronic stroke group models). Scanner was added as an additional control variable in the older adult models to account for potential effects. All predictor variables were mean centered and standardized. To identify which imaging metrics explained the most variance in cognitive performance, we performed model testing of linear regression models by removing the predictor with the smallest beta-value, and comparing model fit with adjusted R^2 and Akaike's information criterion (AIC). We tested for collinearity in predictors by calculating the variance inflation factor (VIF). Separate models were constructed if VIF > 3.0 for any predictors, indicating a high degree of collinearity which may impact the model (Zuur et al., 2010). Because we relied on VIF in our model to indicate covariance we did not test for correlations between TMT performance and DTI or lesion load metrics Final models in this regression analysis were selected if the imaging metric was a significant predictor in the final model, the overall regression model was significant, and the model gave the highest R^2 and lowest AIC in the tested model sets. We estimated effect sizes of predictors in the model with partial η^2.

Once final models were established for TMT performance, we tested whether region-specific imaging metrics or whole-brain lesion volumes explained more variance in TMT performance. We fit a model entering both whole-brain lesion volumes and imaging metrics as predictors. Next, we compared performance between models fit with only whole-brain lesion volumes or regional imaging metrics as predictors.

Finally, we compared model performance between imaging data separated by cerebral hemisphere (left versus right hemisphere for older adult group, ipsilesional versus contralesional for chronic stroke group) to test whether data from one hemisphere explained greater variance in TMT performance. For this analysis we excluded participants with bilateral stroke lesions. We further interrogated the role of hemisphere

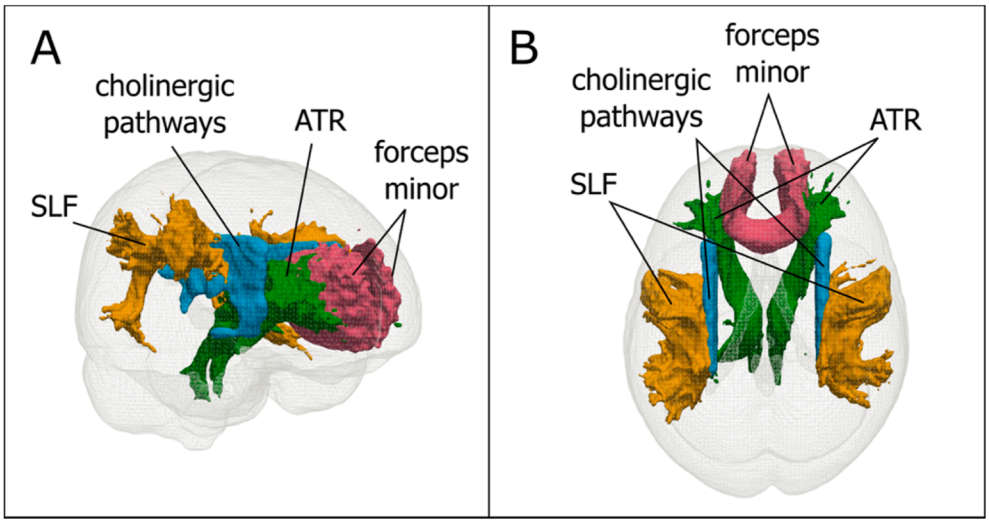

Fig. 2. Overview of regions of interest (ROIs) included in analysis. ROIs included in this manuscript included the anterior thalamic radiations (ATR), cholinergic pathways of the basal forebrain, forceps minor of the corpus callosum, and superior longitudinal fasciculus (SLF). These are visualized in 3D in the sagittal (A) and axial (B) planes.

in TMT performance with a supplementary analysis of individuals with chronic stroke, where we tested relationships between hemispheric imaging data and TMT performance between individuals with left hemisphere versus right hemisphere lesions.

3. Results

We included 62 otherwise healthy older adults and 34 individuals with chronic stroke in this analysis. All participants were successfully processed through MRI processing steps. One older adult was missing DTI imaging, but their lesion load and TMT data was included. One older adult and two individuals with chronic stroke were considered outliers in TMT times (≥3 standard deviations (SDs) above the mean); data from these individuals were excluded from final analyses. Our final sample included 61 older adults (age range: 46–80 years old, 23 males, 56 right-hand dominant) and 32 individuals with chronic stroke (age range: 45–80 years old, 22 males, 7 bilateral stroke infarcts, 13 left hemisphere stroke infarcts, 12 right hemisphere stroke infarcts). In the older adult group, 39 individuals were scanned on the Phillips Achieva MRI, and 22 were scanned on the Phillips Elition MRI. In the chronic stroke group, all 34 individuals were scanned on the Phillips Achieva 3 T MRI.

Table 1 presents participant demographics and mean TMT data for each group. Lesion overlap images for WMHs and stroke lesions are presented in Supplementary Fig. 1. Relative to older adults, the individuals with chronic stroke had lower MoCA scores, larger whole-brain WMH volumes, and a lower proportion of females in the sample. Individuals with chronic stroke also had poorer performance on the TMT indicated by longer total TMT A and TMT B time, and greater differences in time to complete TMT B-A. Supplementary Table 1 presents mean imaging metrics between groups. Relative to older adults, individuals with chronic stroke had significantly lower FA and higher MD in ATR, SLF, and forceps minor (Supplementary Table 1: all $p < 0.001$), and significantly greater WMH lesion load in ATR, SLF, forceps minor and cholinergic pathways (Supplementary Table 1: all $p < 0.010$). We tested for potential sex differences in imaging metrics, presented in Supplementary Tables 2 & Table 3. There were no differences in any imaging metrics between sexes (all p's > 0.05), therefore we did not include sex as a covariate in our statistical models.

Table 1
Participant demographics.

	Older adults	Individuals with chronic stroke	*p*
n	61	32	
Age mean (SD)	64 (9)	66 (8)	0.245†
Sex *n* (%) females	38 (63 %)	10 (31 %)	**0.009**‡
MoCA mean (SD)	27 (2)	25 (3)	**<0.001**†
% ≥23	92 %	84 %	
range	[20–30]	[19–29]	
WMH, mL median (IQR)	0.350 [0.126–1.068]	1.828 [1.126–3.606]	**0.001**†
Stroke lesion, mL median (IQR)	n/a	3.880 [1.260–43.733]	–
Time since stroke mean (SD)	n/a	70 (64)	–
TMT A total (s) mean (SD)	33 (11)	45 (16)	**<0.001**†
TMT B total (s) mean (SD)	51 (17)	83 (46)	**<0.001**†
TMT B-A	18 (14)	38 (37)	**0.003**†
TMT A errors			0.413‡
0	29	17	
1	23	8	
≥2	9	7	
TMT B errors			0.356‡
0	32	14	
1	13	5	
≥2	16	13	

Note: Age is in years and time since stroke is in months, TMT errors is in number of individuals. IQR: interquartile range; SD: standard deviation; s: seconds. Bold values indicate statistical significance ($p < 0.05$). † = group comparison with independent samples *t*-test, ‡ = group comparison with chi-squared test.

3.1. TMT models in older adults

Preliminary spearman's correlations for older adults are presented in

Supplementary Table 4. Bivariate spearman's correlations revealed that total TMT A time significantly correlated with the following variables: ATR FA (r_s = -0.410, p = 0.001), forceps minor FA (r_s = -0.335, p = 0.009), SLF MD (r_s = 0.335, p = 0.009), SLF FA (r_s = -0.289, p = 0.025), and ATR WMH lesion load (r_s = 0.279, p = 0.029). These variables were therefore included in linear regression model testing.

Table 2 presents the final best-fitting models for TMT outcome measures in the older adult group. Full regression model testing is presented in Supplementary Table 5. The best linear regression model fit was achieved by ATR FA as a predictor, which showed a negative relationship with TMT A time after accounting for age and MRI scanner (Table 2). All other imaging variables failed to account for a significant amount of variance in TMT A time, and model performance was improved after these variables were removed (see: Supplementary Table 5).

Bivariate spearman's correlations revealed that total TMT B time was significantly correlated with SLF MD (r_s = 0.387, p = 0.002), but SLF MD did not remain a significant predictor of TMT B time in the linear regression model after accounting for age and MRI scanner (Table 2). TMT B-A time did not significantly correlate with any imaging metrics (all p > 0.05) and therefore did not progress to regression model testing.

3.2. TMT models in individuals with chronic stroke

Preliminary spearman's correlations for older adults are presented in Supplementary Table 6. Bivariate spearman's correlations (r_s) revealed that total TMT A time significantly correlated with the following variables: ATR FA (r_s = -0.460, p = 0.008), ATR MD (r_s = 0.431, p = 0.014), and forceps minor stroke lesion load (r_s = 0.355, p = 0.046). These variables were therefore included in linear regression model testing.

Table 3 presents the final best-fitting models for TMT outcome measures in the chronic stroke group. Full regression model testing is presented for individuals with chronic stroke in Supplementary Table 7. Model testing was performed across two separate models due to high collinearity between ATR FA and MD data (VIF > 4.0). The best linear regression model fit was achieved by ATR MD as a predictor, which showed a negative relationship with total TMT A time, after accounting for age and time since stroke (Table 3). ATR FA was also significantly related to total TMT A time, but the ATR FA model explained less variance in TMT A time than the ATR MD model (adjusted (adj) R^2 ATR FA model: 0.273, vs adj R^2 ATR MD model: 0.390; see Supplementary Table 7).

Bivariate spearman's correlations revealed that total TMT B time was significantly correlated with the following variables: forceps minor MD (r_s = 0.550, p = 0.001), ATR FA (r_s = -0.521, p = 0.002), ATR MD (r_s = 0.477, p = 0.006), forceps minor FA (r_s = -0.376, p = 0.034). These variables were included in linear regression model testing, across two separate models due to high collinearity between FA and MD data (VIF > 4.0). The best linear regression model fit was achieved with ATR FA and forceps minor FA as imaging predictors (Table 3). ATR MD was also a significant predictor of total TMT B time, but the ATR MD model explained less variance in TMT B time than the ATR & forceps minor FA model (adj R^2 ATR & forceps minor FA model: 0.438 vs adj R^2 ATR MD model: 0.304; see Supplementary Table 7).

TMT B-A time was significantly correlated with forceps minor MD (r_s = 0.500, p = 0.004), but forceps minor MD was not a significant predictor of TMT B-A in the linear regression model after accounting for age and time post-stroke (Table 3).

Table 2
Imaging relationsthips with TMT performance in older adults.

	β	VIF	predictor p	R^2	adj R^2	model p
Total TMT A time				**0.378**	**0.294**	**<0.001**
Age	**4.596**	**1.075**	**<0.001**			
Scanner	2.101	1.124	0.418			
ATR FA	**−3.431**	**1.197**	**0.010**			
Total TMT B time				**0.176**	**0.132**	**0.012**
Age	**4.810**	**1.267**	**0.046**			
Scanner	−1.247	1.010	0.776			
SLF MD	3.704	1.256	0.122			

Note: Imaging predictors were entered based on significance in exploratory correlations with outcome measure of interest. Model testing was performed by sequentially removing the imaging predictor with the lowest β-weight and comparing model performance. The presented models are the final models with best performance for each TMT outcome measure, see Supplementary Table 5 for full model testing output. Bold values indicate statistical significance (p < 0.05).

Table 3
Imaging relationships with TMT performance in individuals with chronic stroke.

	β	VIF	predictor p	R^2	adj R^2	model p
Total TMT A time				**0.449**	**0.390**	**< 0.001**
Age	2.062	1.057	0.376			
TSS	−0.044	1.107	0.245			
ATR MD	**11.282**	**1.123**	**<0.001**			
Total TMT B time				**0.511**	**0.438**	**<0.001**
Age	**20.637**	**1.144**	**0.005**			
TSS	−0.073	1.101	0.483			
ATR FA	**−40.485**	**1.740**	**<0.001**			
forceps minor FA	14.740	1.511	0.065			
TMT B-A				0.166	0.076	0.161
Age	8.765	1.042	0.194			
TSS	0.030	1.045	0.774			
forceps minor MD	11.525	1.024	0.088			

Note: Imaging predictors were entered based on significance in exploratory correlations with outcome measure. Model testing was performed by sequentially removing the imaging predictor with the lowest β-weight and comparing model performance. The presented models are the final models with best performance for each TMT outcome measure, see Supplementary Table 7 for full model testing output. TSS: Time since stroke (months). Bold values indicate statistical significance (p < 0.05).

3.3. Region-specific markers versus whole-brain lesion volumes

We tested whether region-specific imaging markers explained more variance in TMT performance compared to whole-brain lesion volumes. We performed model comparison only for TMT measures with significant predictors in the previous linear regression model testing (total TMT A time for older adult group, total TMT A & B time for chronic stroke group). Full model comparisons are presented in Table 4. For every tested TMT outcome measure, regional DTI metrics explained a significant amount of variance in TMT performance over and above whole-brain lesion volumes. Further, the best fitting model in each case was the model with regional DTI metrics only, which provided a better fit to the data then models with whole-brain lesion volumes alone or models with combined whole-brain lesion volumes and regional DTI metrics (see Table 4). In other words, regional DTI metrics explained TMT variance above and beyond whole-brain lesion volumes, and model performance was improved when whole-brain lesion volumes were dropped.

Table 4
Regional imaging metrics versus whole-brain lesion volumes and TMT performance.

Older adults	β	p	partial η^2	R^2	adj R^2	model p	AIC
Total TMT A time							
Both				0.370	0.324	<0.001***	442.629
WMH volume	−0.052	0.973	<0.001				
ATR FA	−3.448	0.016*	0.101				
Whole-brain				0.299	0.261	<0.001***	447.027
WMH volume	1.234	0.410	0.012				
ROI				**0.370**	**0.336**	**<0.001*****	**440.630**
ATR FA	**−3.431**	**0.010***	**0.112**				
Individuals with chronic stroke							
Total TMT A time							
Both				0.456	0.352	0.005**	261.319
WMH volume	1.460	0.579	0.012				
stroke volume	1.304	0.743	0.004				
ATR MD	10.191	0.004**	0.274				
Whole-brain				0.251	0.140	0.089	269.583
WMH volume	4.677	0.101	0.096				
stroke volume	8.758	0.022*	0.180				
ROI				**0.449**	**0.390**	**<0.001*****	**257.760**
ATR MD	**11.282**	**<0.001*****	**0.449**				
Total TMT B time							
Both				0.544	0.434	0.002**	326.198
WMH volume	−3.537	0.661	0.008				
stroke volume	11.197	0.271	0.048				
ATR FA	−40.437	<0.001***	0.401				
forceps minor FA	17.298	0.040*	0.158				
Whole-brain				0.232	0.119	0.117	338.843
WMH volume	12.194	0.145	0.077				
stroke volume	21.251	0.056	0.129				
ROI				**0.511**	**0.438**	**<0.001*****	**324.441**
ATR FA	**−40.485**	**<0.001*****	**0.473**				
forceps minor FA	**14.740**	**0.065**	**0.120**				

Note: Comparing final regression model performance for region-specific imaging metrics against whole-brain lesion volumes (log transformed) in the prediction of TMT performance. Bolded text indicates the model with best performance for each outcome measure. *** = $p < 0.001$; ** = $p < 0.01$; * = $p < 0.05$.

3.4. Hemisphere-specific effects

We tested whether observed TMT relationships with imaging markers were driven by hemisphere effects. For this analysis, we excluded seven participants with bilateral stroke infarcts, leaving a sample size of 25 in the chronic stroke group. We performed model comparison unilateral ATR tracts against TMT measures with significant predictors in the previous linear regression model testing (total TMT A time for older adult group, total TMT A and B time for chronic stroke group). Full model comparisons are presented in Table 5. For the older adult group, both right and left hemisphere ATR FA were significant predictors of TMT A performance, however right hemisphere ATR FA

Table 5
Hemispheric effects of imaging relationships with TMT performance.

Older adults	β	p	partial η^2	R^2	adj R^2	model p	AIC
TMT A							
Left hemisphere				0.359	0.324	<0.001***	441.641
ATR FA	−3.112	0.017*	0.097				
Right hemisphere				**0.370**	**0.336**	**<0.001*****	**440.566**
ATR FA	**−3.528**	**0.010****	**0.113**				
Individuals with chronic stroke							
TMT A							
Contralesional hemisphere				0.164	0.045	0.278	217.961
ATR MD	7.046	0.063	0.155				
Ipsilesional hemisphere				**0.526**	**0.459**	**0.001****	**203.770**
ATR MD	**15.968**	**<0.001*****	**0.521**				
TMT B							
Contralesional hemisphere				0.314	0.177	0.095	268.309
ATR FA	−26.620	0.027*	0.222				
forceps minor FA	3.895	0.733	0.006				
Ipsilesional hemisphere				**0.458**	**0.350**	**0.012***	**262.419**
ATR FA	**−41.665**	**0.002****	**0.385**				
forceps minor FA	**7.998**	**0.430**	**0.031**				

Note: Comparing final regression model performance between hemispheres for unilateral tracts in prediction of TMT performance. Bolded text indicates the model with best performance for each predictor variable. *** = $p < 0.001$; ** = $p < 0.01$; * = $p < 0.05$.

explained more variance in the TMT A data, by a small margin (Table 5; adj R^2 right hemisphere model: 0.336 vs adj R^2 left hemisphere model: 0.324). For the chronic stroke group, only ipsileisonal ATR data related to TMT A and TMT B time, the contralesional hemisphere model did not reach signficance (Table 5).

To further interrogate the role of lesioned hemisphere in the observed DTI-TMT relationships, we conducted a supplementary analysis comparing TMT performance and model fits between individuals with right hemisphere strokes (n = 12) and left hemisphere strokes (n = 13). TMT performance was not different between individuals with right and left hemisphere strokes (Supplementary Table 8; all $p > 0.05$). Within each group, TMT performance related to DTI data from the ipsilesional hemisphere, regardless of whether the ipsilesional hemisphere was a right or left hemispheres lesion (Supplementary Table 9).

4. Discussion

In this study we tested regional white matter markers of processing speed and executive funciton indexed by performance on the TMT. We evaluated multiple frontal-subcortical white matter tracts (ATR, SLF, forceps minor, and cholinergic pathways) using two methods to quantify structural damage in these tracts (regional lesion load and DTI microstructure). This represents a comprehensive evaluation of promising candidate white matter biomarkers that have been identified in previous literature on this topic. Our study has three main findings. First, DTI metrics of the ATR emerged as the best candidate markers of TMT performance for both older adults and individuals with chronic stroke. Second, ATR DTI metrics explained significantly more variance in TMT performance than stroke or WMH volumes from the whole-brain. Third, ipsilesional, but not contralesional, ATR data related to TMT performance in individuals with chronic stroke, whereas both dominant and non-dominant ATR related to TMT performance in older adults.

The development of a cognitive biomarker could facilitate advances in cognitive rehabilitation; a promising, but understudied, area of rehabilitation (Cumming et al., 2013). This study provides encouraging preliminary evidence for ATR microstructure as a candidate biomarker of processing speed and, to a lesser degree, executive function. For context, in the chronic stroke group the effect size of ipsilesional ATR MD with TMT A performance (partial $\eta^2 = 0.526$; Table 5) is comparable to effect sizes seen for ipsilesional corticospinal tract FA and Fugl-Meyer scores (range 0.51–0.62 (Jin et al., 2017), a widely accepted neuroimaging marker of upper extremity motor outcomes post-stroke[7].

4.1. Trail making test and cognition

The TMT is a commonly used cognitive assessment for both healthy and clinical populations and measures multiple components of cognitive performance. For TMT A, we found that higher ATR FA was associated with faster times to complete the TMT A for both older adults and individuals with chronic stroke, although in the chronic stroke group ATR MD explained more variance in TMT A times than ATR FA. We are the first study to show a relationship between ATR microstructure and processing speed in individuals with chronic stroke.

TMT B performance in individuals with chronic stroke was best predicted by a combination of FA from the ATR and forceps minor. Individuals with agenesis of the corpus callosum show deficits in TMT B task performance (Marco, 2012), which may indicate a contribution of interhemispheric communication to the cognitive processes underlying TMT B performance. In our older adult group TMT B performance was not significantly related to any regional imaging measures, which may be explained by the characteristics of our sample. Our older adult sample had very low WMH volumes (mean 1.25 mL, roughly corresponding to a Fazekas score ≤ 1 (van Straaten et al., 2006) and relatively intact cognitive functioning (average MoCA score was 27, 92 % of the sample scored>23 on the MoCA (Carson et al., 2018). Previous studies reporting relationships between ATR structure and TMT B performance in older adults included participants with significantly greater WMH load than the current older adult sample (Duering et al., 2014; MacPherson et al., 2017). Our data are in line with the hypothesis that critical structures for cognitive function become evident only with greater cumulative damage to white matter tracts (Duering et al., 2014) as we observed relationships between ATR microstructure and TMT B performance in the chronic stroke group only.

No white matter tracts emerged as significant predictors of TMT B-A. TMT B-A was the most precise cognitive measure in our battery, and as such it may also require more specific neuroanatomical localization. fMRI studies suggest set-shifting is associated with dorsolateral prefrontal cortex (DLPFC) activity (Moll et al., 2002; Zakzanis et al., 2005). The ATR region encompasses all fibers of the anterior limb of the internal capsule; while this includes projections between the thalamus and DLPFC (Coenen et al., 2012), it also captures projections to other frontal cortex regions including from the medial forebrain bundle (Cho, 2015). It may be that relationships between thalamocortical structure and set-shifting ability will emerge with individualized tractography between the thalamus and DLPFC.

Our findings suggest a relatively greater contribution of ATR microstructure to processing speed rather than set shifting, as ATR microstructure related to TMT A performance across our sample and related to TMT B performance in the chronic stroke group, whereas TMT B-A, a specific measure of set shifting, did not have any significant imaging predictors. Additionally, individuals with chronic stroke took longer to complete TMT-B but did not make more errors relative to the older adult group. This indicates that it is slowed speed, rather than increased set-shifting errors, that contributed to TMT-B performance differences between groups. This argument is supported by Stuss *et al.* who reported that patients with focal frontal lobe lesions and executive dysfunction made more errors on TMT-B, but did not show differences in raw TMT-B completion time (Stuss, 2001; Stuss, 2011). A major theory of aging suggests that slowed processing speed is a central process that underlies poor performance in multiple other cognitive domains (Salthouse, 1996). Our data extend this theory, suggesting that frontal thalamocortical circuitry may be an early mediator of slowed processing speed. Considering the importance of processing speed to multiple components of cognitive abilities (Salthouse, 1996), our findings underscore the potential utility of ATR microstructure for use as a brain-based biomarker of post-stroke cognitive impairment.

4.2. Anterior thalamic radiation

The ATR connects the thalamus and the frontal cortex via the anterior limb of the internal capsule (Hua et al., 2008). The ATR is sensitive to age-related degeneration; in a study of 3,500 adults Cox *et al.* found that the ATR had the largest age-related changes in FA and MD among 14 white matter tracts (Cox, 2016). Similarly, among thalamic grey matter nuclei, regions with frontal cortex connectivity show the most atrophy with aging (Philp et al., 2014). These age-related findings might reflect the vulnerability of the ATR to damage from WMHs, because the anterior limb of the internal capsule travels through the periventricular region of the lateral ventricles, the most common site of WMH formation (Veldsman et al., 2020). The vulnerability of the ATR to WMH formation would explain both the prevalence of processing speed and executive function deficits seen in individuals with WMHs (Vasquez and Zakzanis, 2015), and the structure–function relationships observed in the current study. ATR therefore is a promising candidate marker of cognitive performance, given its widespread connectivity with the frontal lobes (Hua et al., 2008), its vulnerability to age and vascular related degeneration (Cox, 2016), and its relationships with cognitive performance in this and previous (Biesbroek et al., 2016; Biesbroek et al., 2013; Lampe, 2019; Cremers, 2016; MacPherson et al., 2017) reports.

Both left and right hemisphere ATR DTI data related to TMT performance in the older adult group, however only ipsilesional hemisphere ATR FA related to TMT performance in individuals with chronic stroke.

This finding is likely explained by the profound negative impact a stroke has on white matter tracts, which in turn affects cognition. Individuals with chronic stroke had poorer TMT performance compared to older adults with mild WMHs. The effect size for contralesional ATR FA and TMT A performance was similar to the effect sizes observed in both hemispheres for older adults (contralesional partial $\eta 2 = 0.155$ vs left hem partial $\eta 2 = 0.097$; right hem partial $\eta 2 = 0.113$; see Table 5), whereas the effect size for ipsilesional ATR FA was larger in magnitude (partial $\eta 2 = 0.521$). This finding indicates that the damage to white matter caused by a stroke captures a greater amount of variability in TMT performance relative to age-related white matter changes alone. These hemisphere-specific effects of white matter structure in individuals with chronic stroke may indicate that ipsilesional data will provide the most sensitive biomarker of cognitive function, even for cognitive functions without significant hemispheric lateralization.

4.3. DTI-based biomarkers

In this study we employed two methodological indexes of white matter structure to explain variability in TMT performance: DTI and regional lesion load. DTI markers, but not regional lesion load markers, related to TMT performance. ATR DTI microstructure was consistently the best marker across all tested regions and structural metrics, and it related to TMT performance above and beyond whole-brain WMH and stroke volumes. Conversely, region-specific lesion load metrics did not survive regression model testing, and all final models included only DTI metrics.

DTI likely emerged as a sensitive structural marker because DTI can capture more variability in white matter structure than regional lesion volumetrics. In addition to underlying tract anatomy, DTI microstructure is sensitive to both stroke lesions (Reijmer et al., 2013) and WMHs (Muñoz Maniega, 2019). Furthermore, DTI can detect subtle changes to white matter that extend beyond the boundaries of a segmented lesion, such as in the so-called "WMH-penumbra" (Muñoz Maniega, 2019; Ferris, 2022; Maillard et al., 2011) and in stroke-related Wallerian degeneration along the length of tracts (Thomalla et al., 2004). In contrast, lesion volumetrics are based on a binary measure of categorizing a voxel as lesioned or non-lesioned, and thus may miss more subtle effects of lesions on tract structure. In support of this idea, we found that DTI data from the ipsilesional ATR drove relationships with TMT performance, implying that stroke-related damage is involved in the relationship between ATR and TMT performance. However, stroke lesion load in the ATR did not relate to TMT performance, indicating DTI is capturing variability in ATR microstructure above and beyond the stroke lesion that contributes to TMT decline, potentially from co-occurring WMHs. DTI has promise as a clinical tool because it provides a sensitive index of multiple forms of brain damage, and therefore may be useful across a variety of clinical populations. Future research should continue to interrogate the interactions between overt stroke lesions and WMH on behavioural outcomes.

4.4. Limitations

We acknowledge that there are limitations to our study. First, our study was cross-sectional in design; given this we cannot test whether ATR microstructure predicts individual trajectories of cognitive decline. While the cross-sectional design served to explore candidate markers of processing speed and executive functions, future longitudinal studies are needed to evaluate the predictive potential of ATR microstructure for cognitive performance. Second, our study employed a modest sample size, and our findings should be replicated in a larger group of individuals. Third, we employed an atlas-based approach to white matter pathway delineation, which cannot capture individual differences in white matter anatomy. We balanced this limitation by eroding atlas regions to individual white matter anatomy. An atlas-based approach has several strengths, notably it is more easily scalable for clinical translation than individualistic tractography. However, future studies could use individualistic tractography approaches to further probe ATR-TMT relationships, especially to test contributions from specific cortical targets such as DLPFC thalamocortical pathways. Fourth, we do not have information on pre-stroke hand dominance for individuals in the chronic stroke group, and thus cannot speak to how pre-stroke hand dominance may have influenced our results. Finally, it is difficult to disentangle the contributions of processing speed and executive function in cognitive tasks (Albinet et al., 2012), and future studies should more fully investigate the cognitive functions supported by ATR microstructure with a full neuropsychological testing battery.

5. Conclusion

Amongst a group of neuroimaging candidates, ATR microstructure emerged as a robust candidate marker of TMT A performance in older adults and individuals with chronic stroke, and TMT B performance in individuals with chronic stroke. TMT A and TMT B are complex tests that rely on multiple cognitive abilities; however, our data suggest a relatively greater contribution of ATR structure to processing speed, compared to set shifting abilities. ATR microstructure related to TMT performance above and beyond whole-brain WMH and stroke volumes, indicating the importance of regional metrics when considering behavioural relationships. ATR microstructure is a promising candidate for the development of novel markers to predict cognitive decline and response to intervention in cerebrovascular disease.

CRediT authorship contribution statement

Jennifer Ferris: Conceptualization, Investigation, Methodology, Formal analysis, Writing – original draft, Writing – review & editing. **Brian Greeley:** Investigation, Writing – review & editing. **Negin Motamed Yeganeh:** Investigation, Writing – review & editing. **Shie Rinat:** Investigation, Writing – review & editing. **Joel Ramirez:** Methodology, Writing – review & editing. **Sandra Black:** Methodology, Writing – review & editing. **Lara Boyd:** Supervision, Investigation, Writing – review & editing, Funding acquisition, Project administration.

Declaration of Competing Interest

The authors declare that they have no known competing financial interests or personal relationships that could have appeared to influence the work reported in this paper.

Data availability

Data will be made available on request.

Acknowledgements

We gratefully acknowledge the assistance of imaging analysts in the LC Campbell Cognitive Neurology Research Unit, including Sabrina Adamo, Miracle Ozzude, Dr. Fuqiang Gao, and Christopher Scott. We thank Dr. Teresa Liu Ambrose for helpful conversations related to this paper. Funding was provided by the Canadian Institutes of Health Research (MOP-130269, PTJ-148535 and PTJ-153330; PI Boyd).

Appendix A. Supplementary data

Supplementary data to this article can be found online at https://doi.org/10.1016/j.nicl.2022.103174.

References

Albinet, C.T., Boucard, G., Bouquet, C.A., Audiffren, M., 2012. Processing speed and executive functions in cognitive aging: How to disentangle their mutual relationship? Brain Cogn. 79, 1–11.

Andersson, J.L.R., Jenkinson, M., Smith, S., 2007. Non-linear registration aka spatial normalisation. FMRIB Technical Report TR07JA2.

Arsava, E.M., Rahman, R., Rosand, J., Lu, J., Smith, E.E., Rost, N.S., Singhal, A.B., Lev, M. H., Furie, K.L., Koroshetz, W.J., Sorensen, A.G., Ay, H., 2009. Severity of leukoaraiosis correlates with clinical outcome after ischemic stroke. Neurology 72 (16), 1403–1410.

Ballinger, E., Ananth, M., Talmage, D., Role, L., 2016. Basal Forebrain Cholinergic Circuits and Signaling in Cognition and Cognitive Decline. Neuron 91 (6), 1199–1218.

Barker-Collo, S., Feigin, V.L., Parag, V., Lawes, C.M.M., Senior, H., 2010. Auckland Stroke Outcomes Study: Part 2: Cognition and functional outcomes 5 years poststroke. Neurology 75 (18), 1608–1616.

Biesbroek, J.M., Kuijf, H.J., van der Graaf, Y., Vincken, K.L., Postma, A., Mali, W.P.T.M., Biessels, G.J., Geerlings, M.I., Scuteri, A., 2013. Association between Subcortical Vascular Lesion Location and Cognition: A Voxel-Based and Tract-Based Lesion-Symptom Mapping Study. The SMART-MR Study. *PLoS One* 8 (4), e60541.

Biesbroek, J.M., Weaver, N.A., Hilal, S., Kuijf, H.J., Ikram, M.K., Xu, X., Tan, B.Y., Venketasubramanian, N., Postma, A., Biessels, G.J., Chen, C.P.L.H., Ginsberg, S.D., 2016. Impact of Strategically Located White Matter Hyperintensities on Cognition in Memory Clinic Patients with Small Vessel Disease. PLoS One 11 (11), e0166261.

Bocti, C., Swartz, R.H., Gao, F.-Q., Sahlas, D.J., Behl, P., Black, S.E., 2005. A new visual rating scale to assess strategic white matter hyperintensities within cholinergic pathways in dementia. Stroke 36 (10), 2126–2131.

Bowie, C.R., Harvey, P.D., 2006. Administration and interpretation of the Trail Making Test. Nat. Protoc. 1, 2277–2281.

Boyd, L.A., Hayward, K.S., Ward, N.S., Stinear, C.M., Rosso, C., Fisher, R.J., Carter, A.R., Leff, A.P., Copland, D.A., Carey, L.M., Cohen, L.G., Basso, D.M., Maguire, J.M., Cramer, S.C., 2017. Biomarkers of Stroke Recovery: Consensus-Based Core Recommendations from the Stroke Recovery and Rehabilitation Roundtable. Int. J. Stroke 12 (5), 480–493.

Carson, N., Leach, L., Murphy, K.J., 2018. A re-examination of Montreal Cognitive Assessment (MoCA) cutoff scores. Int. J. Geriatr. Psychiatry 33, 379–388.

Cho, Z. H. *et al.* An anatomic review of thalamolimbic fiber tractography: Ultra-high resolution direct visualization of thalamolimbic fibers anterior thalamic radiation, superolateral and inferomedial medial forebrain bundles, and newly identified septum pellucidum tract. *World Neurosurg.* 83, 54-61.E32 (2015).

Coenen, V.A., Panksepp, J., Hurwitz, T.A., Urbach, H., Mädler, B., 2012. Human medial forebrain bundle (MFB) and anterior thalamic radiation (ATR): Imaging of two major subcortical pathways and the dynamic balance of opposite affects in understanding depression. J. Neuropsychiatry Clin. Neurosci. 24, 223–236.

Cox, S.R., et al., 2016. Ageing and brain white matter structure in 3,513 UK Biobank participants. Nat. Commun. 7, 1–13.

Cremers, L.G.M., et al., 2016. Altered tract-specific white matter microstructure is related to poorer cognitive performance: The Rotterdam Study. Neurobiol. Aging 39, 108–117.

Crowe, S.F., 1998. The differential contribution of mental tracking, cognitive flexibility, visual search, and motor speed to performance on parts A and B of the trail making test. J. Clin. Psychol. 54 (5), 585–591.

Cumming, T.B., Marshall, R.S., Lazar, R.M., 2013. Stroke, cognitive deficits, and rehabilitation: Still an incomplete picture. Int. J. Stroke 8 (1), 38–45.

Dade, L.A., Gao, F.Q., Kovacevic, N., Roy, P., Rockel, C., O'Toole, C.M., Lobaugh, N.J., Feinstein, A., Levine, B., Black, S.E., 2004. Semiautomatic brain region extraction: A method of parcellating brain regions from structural magnetic resonance images. Neuroimage 22 (4), 1492–1502.

Debette, S., Markus, H.S., 2010. The clinical importance of white matter hyperintensities on brain magnetic resonance imaging: Systematic review and meta-analysis. BMJ 341 (jul26 1), c3666–c.

Devos, H., Akinwuntan, A.E., Nieuwboer, A., Truijen, S., Tant, M., De Weerdt, W., 2011. Screening for fitness to drive after stroke: A systematic review and meta-analysis. Neurology 76 (8), 747–756.

Duering, M. *et al.* Strategic role of frontal white matter tracts in vascular cognitive impairment: A voxel-based lesion-symptom mapping study in CADASIL. *Brain* 134, 2366–2375 (2011).

Duering, M., Gonik, M., Malik, R., Zieren, N., Reyes, S., Jouvent, E., Hervé, D., Gschwendtner, A., Opherk, C., Chabriat, H., Dichgans, M., 2013. Identification of a strategic brain network underlying processing speed deficits in vascular cognitive impairment. Neuroimage 66, 177–183.

Duering, M., Gesierich, B., Seiler, S., Pirpamer, L., Gonik, M., Hofer, E., Jouvent, E., Duchesnay, E., Chabriat, H., Ropele, S., Schmidt, R., Dichgans, M., 2014. Strategic white matter tracts for processing speed deficits in age-related small vessel disease. Neurology 82 (22), 1946–1950.

Ewers, M., et al., 2012. Prediction of conversion from mild cognitive impairment to Alzheimer's disease dementia based upon biomarkers and neuropsychological test performance. Neurobiol. Aging 33, 1203–1214.

Feng, W., et al., 2015. Corticospinal Tract Lesion Load - A Potential Imaging Biomarker for Stroke Motor Outcomes. Ann. Neurol. 78, 860–870.

Ferris, J. K. *et al.* In vivo myelin imaging and tissue microstructure in white matter hyperintensities and perilesional white matter. *Brain Commun.* In press, (2022).

Hua, K., Zhang, J., Wakana, S., Jiang, H., Li, X., Reich, D.S., Calabresi, P.A., Pekar, J.J., van Zijl, P.C.M., Mori, S., 2008. Tract Probability Maps in Stereotaxic Spaces: Analyses of White Matter Anatomy and Tract-Specific Quantification. Neuroimage 39 (1), 336–347.

Jeerakathil, T., Wolf, P.A., Beiser, A., Massaro, J., Seshadri, S., D'Agostino, R.B., DeCarli, C., 2004. Stroke risk profile predicts white matter hyperintensity volume: The Framingham study. Stroke 35 (8), 1857–1861.

Jenkinson, M., Bannister, P., Brady, M., Smith, S., 2002. Improved Optimization for the Robust and Accurate Linear Registration and Motion Correction of Brain Images. Neuroimage 17 (2), 825–841.

Jin, J., Guo, Z., Zhang, Y., Chen, Y., 2017. Prediction of motor recovery after ischemic stroke using diffusion tensor imaging: A meta-analysis. World J. Emerg. Med. 8, 99.

Knopman, D.S., et al., 2009. Association of Prior Stroke with Cognitive Function and Cognitive Impairment: A Population-based Study. Arch. Neurol. 66, 614–619.

Lampe, L., et al., 2019. Lesion location matters: The relationships between white matter hyperintensities on cognition in the healthy elderly. J. Cereb. Blood Flow Metab. 39, 36–43.

Lim, J.-S., Kim, N., Jang, M.U., Han, M.-K., Kim, SangYun, Baek, M.J., Jang, M.S., Ban, B., Kang, Y., Kim, D.-E., Lee, J.S., Lee, J., Lee, B.-C., Yu, K.-H., Black, S.E., Bae, H.-J., 2014. Cortical Hubs and Subcortical Cholinergic Pathways as Neural Substrates of Poststroke Dementia. Stroke 45 (4), 1069–1076.

MacPherson, S.E., Cox, S.R., Dickie, D.A., Karama, S., Starr, J.M., Evans, A.C., Bastin, M. E., Wardlaw, J.M., Deary, I.J., 2017. Processing speed and the relationship between Trail Making Test-B performance, cortical thinning and white matter microstructure in older adults. Cortex 95, 92–103.

Mahon, S., et al., 2020. Slowed Information Processing Speed at Four Years Poststroke: Evidence and Predictors from a Population-Based Follow-up Study. J. Stroke Cerebrovasc. Dis. 29, 104513.

Maillard, P., Fletcher, E., Harvey, D., Carmichael, O., Reed, B., Mungas, D., DeCarli, C., 2011. White matter hyperintensity penumbra. Stroke 42 (7), 1917–1922.

Mang, C.S., Whitten, T.A., Cosh, M.S., Scott, S.H., Wiley, J.P., Debert, C.T., Dukelow, S. P., Benson, B.W., Tzekov, R., 2018. Test-retest reliability of the KINARM end-point robot for assessment of sensory, motor and neurocognitive function in young adult athletes. PLoS One 13 (4), e0196205.

Mang, C.S., Whitten, T.A., Cosh, M.S., Scott, S.H., Wiley, J.P., Debert, C.T., Dukelow, S. P., Benson, B.W., 2019. Robotic Assessment of Motor, Sensory, and Cognitive Function in Acute Sport-Related Concussion and Recovery. J. Neurotrauma 36 (2), 308–321.

Marco, E.J., et al., 2012. Processing speed delays contribute to executive function deficits in individuals with agenesis of the corpus callosum. J. Int. Neuropsychol. Soc. 18, 521–529.

McNeely, A.A., et al., 2015. Cholinergic subcortical hyperintensities in Alzheimer's disease patients from the Sunnybrook dementia study: Relationships with cognitive dysfunction and hippocampal atrophy. J. Alzheimer's Dis. 43, 785–796.

Moll, J., De Oliveira-Souza, R., Moll, F.T., Bramati, I.E., Andreiuolo, P.A., 2002. The cerebral correlates of set-shifting: An fMRI study of the trail making test. Arq. Neuropsiquiatr. 60, 900–905.

Muir, R.T., Lam, B., Honjo, K., Harry, R.D., McNeely, A.A., Gao, F.-Q., Ramirez, J., Scott, C.J.M., Ganda, A., Zhao, J., Zhou, X.J., Graham, S.J., Rangwala, N., Gibson, E., Lobaugh, N.J., Kiss, A., Stuss, D.T., Nyenhuis, D.L., Lee, B.-C., Kang, Y., Black, S.E., 2015. Trail making test elucidates neural substrates of specific poststroke executive dysfunctions. Stroke 46 (10), 2755–2761.

Muñoz Maniega, S., et al., 2019. Spatial Gradient of Microstructural Changes in Normal-Appearing White Matter in Tracts Affected by White Matter Hyperintensities in Older Age. Front. Neurol. 10, 1–14.

Nachev, P., Coulthard, E., Jäger, H.R., Kennard, C., Husain, M., 2008. Enantiomorphic normalization of focally lesioned brains. Neuroimage 39 (3), 1215–1226.

Narasimhalu, K., Ang, S., De Silva, D.A., Wong, M.-C., Chang, H.-M., Chia, K.-S., Auchus, A.P., Chen, C.P., 2011. The prognostic effects of poststroke cognitive impairment no dementia and domain-specific cognitive impairments in nondisabled ischemic stroke patients. Stroke 42 (4), 883–888.

Nasreddine, Z., et al., 2005. Montreal Cognitive Assessment (MoCA) Administration, Administration and Scoring Instructions. J. Am. Geriatr. Soc. 53, 695–699.

Perry, M.E., McDonald, C.R., Hagler, D.J., Gharapetian, L., Kuperman, J.M., Koyama, A. K., Dale, A.M., McEvoy, L.K., 2009. White matter tracts associated with set-shifting in healthy aging. Neuropsychologia 47 (13), 2835–2842.

Philp, D.J., Korgaonkar, M.S., Grieve, S.M., 2014. Thalamic volume and thalamo-cortical white matter tracts correlate with motor and verbal memory performance. Neuroimage 91, 77–83.

Pohjasvaara, T., et al., 2002. Post-stroke depression, executive dysfunction and functional outcome. Eur. J. Neurol. 9, 269–275.

Ramirez, J., Gibson, E., Quddus, A., Lobaugh, N.J., Feinstein, A., Levine, B., Scott, C.J.M., Levy-Cooperman, N., Gao, F.Q., Black, S.E., 2011. Lesion Explorer: A comprehensive segmentation and parcellation package to obtain regional volumetrics for subcortical hyperintensities and intracranial tissue. Neuroimage 54 (2), 963–973.

Ramirez, J., Holmes, M.F., Scott, C.J.M., Ozzoude, M., Adamo, S., Szilagyi, G.M., Goubran, M., Gao, F., Arnott, S.R., Lawrence-Dewar, J.M., Beaton, D., Strother, S.C., Munoz, D.P., Masellis, M., Swartz, R.H., Bartha, R., Symons, S., Black, S.E., 2020. Ontario Neurodegenerative Disease Research Initiative (ONDRI): Structural MRI Methods and Outcome Measures. Front. Neurol. 11.

Rasmusson, D.X., Zonderman, A.B., Kawas, C., Resnick, S.M., 1998. Effects of age and dementia on the trail making test. Clin. Neuropsychol. 12, 169–178.

Reijmer, Y.D., Freeze, W.M., Leemans, A., Biessels, G.J., 2013. The effect of lacunar infarcts on white matter tract integrity. Stroke 44 (7), 2019–2021.

Salthouse, T.A., 1996. The Processing-Speed Theory of Adult Age Differences in Cognition. Psychol. Rev. 103, 403–428.

Schear, J.M., Sato, S.D., 1989. Effects of visual acuity and visual motor speed and dexterity on cognitive test performance. Arch. Clin. Neuropsychol. 4, 25–32.

Scott, S.H., Dukelow, S.P., 2011. Potential of robots as next-generation technology for clinical assessment of neurological disorders and upper-limb therapy. J. Rehabil. Res. Dev. 48, 335–354.
Selden, N.R., Gitelman, D.R., Salamon-Murayama, N., Parrish, T.B., Mesulam, M.M., 1998. Trajectories of cholinergic pathways within the cerebral hemispheres of the human brain. Brain 121, 2249–2257.
Sexton, E., et al., 2019. Systematic review and meta-analysis of the prevalence of cognitive impairment no dementia in the first year post-stroke. Eur. Stroke J. 4, 160–171.
Smith, S.M., 2002. Fast robust automated brain extraction. Hum. Brain Mapp. 17 (3), 143–155.
Smith, S.M., Jenkinson, M., Woolrich, M.W., Beckmann, C.F., Behrens, T.E.J., Johansen-Berg, H., Bannister, P.R., De Luca, M., Drobnjak, I., Flitney, D.E., Niazy, R.K., Saunders, J., Vickers, J., Zhang, Y., De Stefano, N., Brady, J.M., Matthews, P.M., 2004. Advances in functional and structural MR image analysis and implementation as FSL. Neuroimage 23, S208–S219.
Stuss, D.T., et al., 2001. The Trail Making Test: A study in focal lesion patients. Psychol. Assess. 13, 230–239.
Stuss, D.T., 2011. Functions of the frontal lobes: Relation to executive functions. J. Int. Neuropsychol. Soc. 17 (05), 759–765.
Tekin, S., Cummings, J.L., 2002. Frontal-subcortical neuronal circuits and clinical neuropsychiatry: An update. J. Psychosom. Res. 53, 647–654.
Thomalla, G., Glauche, V., Koch, M.A., Beaulieu, C., Weiller, C., Röther, J., 2004. Diffusion tensor imaging detects early Wallerian degeneration of the pyramidal tract after ischemic stroke. Neuroimage 22 (4), 1767–1774.
Tombaugh, T., 2004. Trail Making Test A and B: Normative data stratified by age and education. Arch. Clin. Neuropsychol. 19 (2), 203–214.
van Straaten, E.C.W., Fazekas, F., Rostrup, E., Scheltens, P., Schmidt, R., Pantoni, L., Inzitari, D., Waldemar, G., Erkinjuntti, T., Mäntylä, R., Wahlund, L.-O., Barkhof, F., 2006. Impact of white matter hyperintensities scoring method on correlations with clinical data: The LADIS study. Stroke 37 (3), 836–840.
Vasquez, B.P., Zakzanis, K.K., 2015. The neuropsychological profile of vascular cognitive impairment not demented: A meta-analysis. J. Neuropsychol. 9, 109–136.
Veldsman, M., Kindalova, P., Husain, M., Kosmidis, I., Nichols, T.E., 2020. Spatial distribution and cognitive impact of cerebrovascular risk-related white matter hyperintensities. NeuroImage Clin. 28, 102405.
Veldsman, M., Werden, E., Egorova, N., Khlif, M.S., Brodtmann, A., 2020. Microstructural degeneration and cerebrovascular risk burden underlying executive dysfunction after stroke. Sci. Rep. 10, 1–8.
Wen, W., Sachdev, P.S., 2004. Extent and distribution of white matter hyperintensities in stroke patients: The Sydney Stroke Study. Stroke 35 (12), 2813–2819.
Zakzanis, K.K., Mraz, R., Graham, S.J., 2005. An fMRI study of the Trail Making Test. Neuropsychologia 43 (13), 1878–1886.
Zuur, A.F., Ieno, E.N., Elphick, C.S., 2010. A protocol for data exploration to avoid common statistical problems. Methods Ecol. Evol. 1, 3–14.